

Spin qubits in graphene quantum dots

Björn Trauzettel, Denis V. Bulaev, Daniel Loss, and Guido Burkard

Department of Physics and Astronomy, University of Basel, Klingelbergstrasse 82, CH-4056 Basel, Switzerland

(Dated: November 2006)

We propose how to form spin qubits in graphene. A crucial requirement to achieve this goal is to find quantum dot states where the usual valley degeneracy in bulk graphene is lifted. We show that this problem can be avoided in quantum dots based on ribbons of graphene with semiconducting armchair boundaries. For such a setup, we find the energies and the exact wave functions of bound states, which are required for localized qubits. Additionally, we show that spin qubits in graphene can not only be coupled between nearest neighbor quantum dots via Heisenberg exchange interaction but also over long distances. This remarkable feature is a direct consequence of the quasi-relativistic spectrum of graphene.

PACS numbers: 67.57.Lm, 73.21.La, 74.78.Na

The electron spin is a very promising candidate for a solid-state qubit [1]. Major experimental breakthroughs have been achieved in recent years using quantum dots formed in semiconductor heterostructures based on GaAs technology [2, 3, 4, 5]. In such devices, the major sources of spin decoherence have been identified as the spin-orbit interaction, coupling the spin to lattice vibrations [6], and the hyperfine interaction of the electron spin with the surrounding nuclear spins [7, 8, 9, 10, 11]. Therefore, it is desirable to form qubits in quantum dots based on other materials, where spin-orbit coupling and hyperfine interaction are considerably weaker [12]. It is well known that carbon-based materials such as nanotubes or graphene are excellent candidates. This is so because spin-orbit coupling is weak in carbon due to its relatively low atomic weight, and because natural carbon consists predominantly of the zero-spin isotope ^{12}C , for which the hyperfine interaction is absent.

Here we show how to form spin qubits in graphene. A crucial requirement to achieve this goal is to find quantum dot states where the usual valley degeneracy is lifted. We show that this problem can be avoided in quantum dots with so-called armchair boundaries. We furthermore show that spin qubits in graphene can not only be coupled (via Heisenberg exchange) between nearest neighbor quantum dots but also over long distances. This remarkable feature is a direct consequence of the Klein paradox being a distinct feature of the quasi-relativistic spectrum of graphene. Therefore, the proposed system is ideal for fault-tolerant quantum computation, and thus for scalability, since it offers a low error rate due to weak decoherence, in combination with a high error threshold due to the possibility of long-range coupling.

Only very recently, the fabrication of a single layer of graphene and the measurement of its electric transport properties have been achieved [13, 14, 15]. Two fundamental problems need to be overcome before graphene can be used to form spin qubits and to operate one or two of them as proposed in Refs. [1, 7]: (i) It is difficult to create a tunable quantum dot in graphene because of the absence of a gap in the spectrum. The phenomenon of Klein tunneling makes it hard to confine particles [16, 17, 18]. (ii) Due to the valley degeneracy that exists in graphene [19, 20, 21], it is non-trivial to form two-qubit gates using Heisenberg exchange coupling for spins in tunnel-coupled dots. Several attempts have been made to

solve the problem (i) such as to use suitable transverse states in graphene ribbons to confine electrons [22], to combine single and bilayer regions of graphene [23], or to achieve confinement by using inhomogeneous magnetic fields [24]. The problem (ii) has not been recognized up to now. Here we propose a setup which solves both problems (i) and (ii) at once. Similar to Ref. [22] we choose to confine electrons by using suitable transverse states in a ribbon of graphene, *cf.* Fig. 1. In particular, we assume *semiconducting armchair* boundary conditions to exist on two opposite edges of the sample. It is known that in such a device the valley degeneracy is lifted [25, 26], which is the essential prerequisite for the appearance of Heisenberg exchange coupling for spins in tunnel-coupled quantum dots (see below), and thus for the use of graphene dots for spin qubits. We show below that spin qubits in graphene can not only be coupled between nearest neighbor quantum dots but also over long distances. This long-distance coupling mechanism makes use of conduction band to valence band tunneling processes and is, therefore, directly based on the Klein paradox in graphene [17, 18].

We now discuss bound-state solutions in our setup, which are required for a localized qubit. We first concentrate on a single quantum dot which is assumed to be rectangular with width W and length L , see Fig. 1. The basic idea of forming the dot is to take a ribbon of graphene with semiconducting armchair boundary conditions in x -direction and to electrically confine particles in y -direction. The low energy properties of electrons (with energy ε with respect to the Dirac point) in such a setup are described by the 4x4 Dirac equation

$$-i\hbar v \begin{pmatrix} \sigma_x \partial_x + \sigma_y \partial_y & 0 \\ 0 & -\sigma_x \partial_x + \sigma_y \partial_y \end{pmatrix} \Psi + eV(y)\Psi = \varepsilon\Psi, \quad (1)$$

where the electric gate potential is assumed to vary stepwise, $V(y) = V_{\text{gate}}$ in the dot region (where $0 \leq y \leq L$), and $V(y) = V_{\text{barrier}}$ in the barrier region (where $y < 0$ or $y > L$). In Eq. (1), σ_x and σ_y are Pauli matrices and v is the Fermi velocity. The four component spinor envelope wave function $\Psi = (\Psi_A^{(K)}, \Psi_B^{(K)}, -\Psi_A^{(K')}, -\Psi_B^{(K')})$ varies on scales large compared to the lattice spacing [28]. Here, A and B refer to the two sublattices in the two-dimensional honeycomb lattice of carbon atoms, whereas K and K' refer to the vectors in reciprocal space corresponding to the two valleys in the bandstructure of

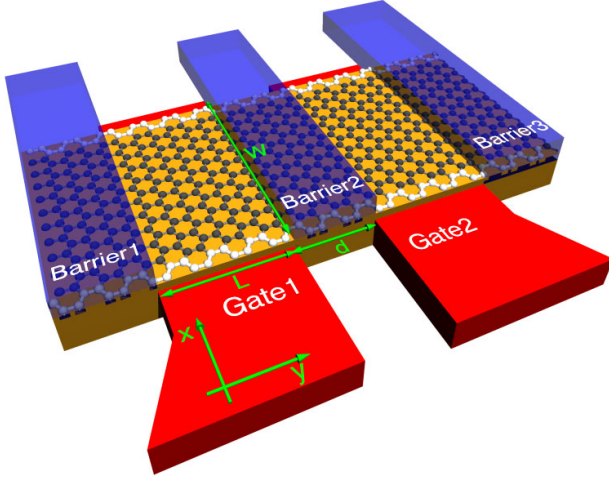


FIG. 1: Schematic of a graphene double quantum dot. Each dot is assumed to have length L and width W . The structure is based on a ribbon of graphene (grey) with semiconducting armchair edges (white). Confinement is achieved by tuning the voltages applied to the ‘‘barrier’’ gates (blue) to appropriate values such that bound states exist. Additional gates (red) allow to shift the energy levels of the dots. Virtual hopping of electrons through barrier 2 (thickness d) gives rise to a tunable exchange coupling J between two electron spins localized in the left and the right dot. The exchange coupling is then used to generate universal two-qubit gates.

graphene. The appropriate semiconducting armchair boundary conditions for such a wave function have been formulated in Ref. [25] and can be written as ($\alpha = A, B$)

$$\Psi_{\alpha}^{(K)}|_{x=0} = \Psi_{\alpha}^{(K')}|_{x=0}, \quad \Psi_{\alpha}^{(K)}|_{x=W} = e^{\pm 2\pi/3} \Psi_{\alpha}^{(K')}|_{x=W}, \quad (2)$$

corresponding to a width W of the ribbon shown in Fig. 1, where W is not an integer multiple of three unit cells. The \pm signs in Eq. (2) (as well as in Eq. (3) below) correspond to the two possible choices of a number of unit cells that is not an integer multiple of three. The full set of plane wave solutions of Eq. (1) is readily determined [26]. It is well known that the boundary condition (2) yields the following quantization conditions for the wave vector $k_x \equiv q_n$ in x -direction [25, 26]

$$q_n = (n \pm 1/3)\pi/W, \quad n \in \mathbb{Z}. \quad (3)$$

The level spacing associated with the quantization conditions (3) can be estimated as $\Delta\epsilon \approx \hbar v\pi/3W$, which gives $\Delta\epsilon \approx 30$ meV, where we used that $v \approx 10^6$ m/s and assumed a quantum dot width of about $W \approx 30$ nm. Note that Eq. (3) also determines the energy gap for excitations as $E_{\text{gap}} = 2\hbar v q_0$. Therefore, this gap is of the order of 60 meV, which is unusually small for semiconductors. This is a unique feature of graphene that will allow long-distance coupling of spin qubits as will be discussed below Eq. (10).

We now discuss in more detail the ground-state wave function corresponding to the case $n = 0$ in Eq. (3). The ground-state solution is independent of whether the crystall structure dictates the $+$ or the $-$ sign in Eqs. (2) and (3) and can be

written as

$$\Psi_0(x, y) = \begin{cases} \alpha_0 \chi_{0,k}^{(-)}(x) e^{-iky}, & \text{if } y < 0, \\ \beta_0 \chi_{0,k}^{(+)}(x) e^{iky} + \gamma_0 \chi_{0,k}^{(-)}(x) e^{-iky}, & \text{if } 0 \leq y \leq L, \\ \delta_0 \chi_{0,k}^{(+)}(x) e^{ik(y-L)}, & \text{if } y > L, \end{cases} \quad (4)$$

where $\chi_{0,k}^{(+)}(x) = (e^{iq_0 x}, z_{0,k} e^{iq_0 x}, e^{-iq_0 x}, z_{0,k} e^{-iq_0 x})$ and $\chi_{0,k}^{(-)}(x) = (z_{0,k} e^{iq_0 x}, e^{iq_0 x}, z_{0,k} e^{-iq_0 x}, e^{-iq_0 x})$. In Eq. (4), the coefficients α_0 , β_0 , γ_0 , and δ_0 are determined (up to a normalization constant) for a specific bound-state solution to Eq. (1) and

$$z_{0,k} \equiv \pm \frac{q_0 + ik}{\sqrt{q_0^2 + k^2}}, \quad (5)$$

where $k_y \equiv k$ is the wave vector in y -direction. In Eq. (5), the \pm sign refers to a conduction band (+) and a valence band (-) solution to Eq. (1). The corresponding ground-state energy ϵ can be expressed relative to the potential barrier $V = V_{\text{barrier}}$ in the regions $y < 0$ and $y > L$ as $\epsilon = eV_{\text{barrier}} \pm \hbar v(q_0^2 + k^2)^{1/2}$. For bound states to exist and to decay at $y \rightarrow \pm\infty$, we require that $\hbar v q_0 > |\epsilon - eV_{\text{barrier}}|$, which implies that

$$k = i \sqrt{q_0^2 - ((\epsilon - eV_{\text{barrier}})/\hbar v)^2}, \quad (6)$$

is purely imaginary. In the dot region ($0 \leq y \leq L$), the wave vector k in y -direction is replaced by \tilde{k} , satisfying $\epsilon = eV_{\text{gate}} \pm \hbar v(q_0^2 + \tilde{k}^2)^{1/2}$. Again the \pm sign refers to conduction and valence band solutions. In the following, we focus on conduction band solutions to the problem.

Since the Dirac equation (1) implies the continuity of the wave function, the matching condition at $y = 0$ and $y = L$ allows us to derive the transcendental equation for ϵ

$$e^{2i\tilde{k}L} (z_{0,k} - z_{0,\tilde{k}})^2 - (1 - z_{0,k} z_{0,\tilde{k}})^2 = 0. \quad (7)$$

This equation determines the allowed energies ϵ for bound states. In order to analyze the solutions to Eq. (7), we distinguish two cases, one where \tilde{k} is real, and the other, where \tilde{k} is purely imaginary. The two cases are distinguished by the condition $|\epsilon - eV_{\text{gate}}| \geq \hbar v q_0$ and $|\epsilon - eV_{\text{gate}}| < \hbar v q_0$, respectively. Furthermore, we assume that $V_{\text{gate}} \neq V_{\text{barrier}}$, i.e., $z_{0,k} \neq z_{0,\tilde{k}}$ [29]. In the case, where \tilde{k} is purely imaginary, there is no bound-state solution. This is due to the fact that such a solution would have to exist directly in the bandgap. We now analyze solutions for real \tilde{k} . In the corresponding energy window

$$|\epsilon - eV_{\text{gate}}| \geq \hbar v q_0 > |\epsilon - eV_{\text{barrier}}|, \quad (8)$$

we can simplify Eq. (7) considerably, obtaining

$$\tan(\tilde{k}L) = \frac{\hbar v \tilde{k} \sqrt{(\hbar v q_0)^2 - (\epsilon - eV_{\text{barrier}})^2}}{(\epsilon - eV_{\text{barrier}})(\epsilon - eV_{\text{gate}}) - (\hbar v q_0)^2}. \quad (9)$$

We show a set of solutions to Eq. (9) for a relatively short dot ($q_0 L = 2$) as well as a longer dot ($q_0 L = 5$) in Fig. 2. The number of bound states N (for $n = 0$) is maximal if $\Delta V = V_{\text{barrier}} - V_{\text{gate}}$ is exactly as large as the size of the gap

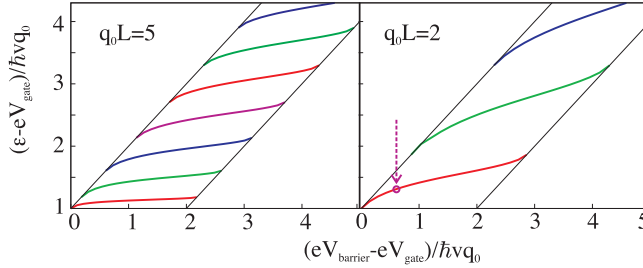


FIG. 2: Bound-state solutions of a relatively long ($q_0L = 5$, left panel) and a shorter ($q_0L = 2$, right panel) quantum dot are shown. The diagonal straight lines mark the area in which bound-state solutions can occur. The arrow marks the solution, for which the wave function is plotted in Fig. 4.

$E_{\text{gap}} = 2\hbar\nu q_0$, then $N_{\text{max}} = \lceil \sqrt{8}q_0L/\pi \rceil$, where $\lceil x \rceil$ is the integer just larger than x . The level spacing associated with the allowed solutions of Eq. (9) increases as L decreases and has a rather complicated parameter dependence. It can, however, be estimated to be of the order of $\Delta\epsilon \approx \hbar\nu\pi/\max\{W, L\}$, which is in the energy range of a few tens of meV as mentioned below Eq. (3). In Fig. 3, we show the energy bands of a single dot and two neighboring barrier regions as well as a double dot setup with three barrier regions. The double dot case illustrates how we make use of the Klein paradox to couple two dots.

A particular example of a wave function is shown in Fig. 4. It is a ground-state solution under the parameter choice $e(V_{\text{barrier}} - V_{\text{gate}}) = 0.6\hbar\nu q_0$, and $q_0L = 2$ (indicated by the arrow in Fig. 2). The weight of the wave function on the A and B lattice sites is different, however, the integrated weight is the same as required by the normalization condition [25]. Ground-state solutions (i.e. the lowest lying (red) lines in Fig. 2) have no nodes in the dot region – similar to the corresponding problem of confined electrons that obey the non-relativistic Schrödinger equation. Excited-state solutions in parameter regions in which they exist, do have nodes in the dot region (not shown here).

We now turn to the case of two coupled graphene quantum dots, separated by a potential barrier, as sketched in Fig. 1, each dot filled with a single electron. It is interesting to ask whether the spins \mathbf{S}_i of these two electrons ($i = 1, 2$) are coupled through an exchange coupling, $H_{\text{exch}} = \mathbf{J}\mathbf{S}_1 \cdot \mathbf{S}_2$, in the same way as for regular semiconductor quantum dots [7], because this coupling is, in combination with single-spin rotations, sufficient to generate all quantum gates required for universal quantum computation [1]. The exchange coupling is based on the Pauli exclusion principle which allows for electron hopping between the dots in the spin singlet state (with opposite spins) of two electrons, but not in a spin triplet (with parallel spins), thus leading to a singlet-triplet splitting (exchange energy) J . However, a singlet-triplet splitting $J \neq 0$ only occurs if the triplet state with two electrons on the same dot in the ground state is forbidden, i.e., in the case of a single *non-degenerate* orbital level. This is

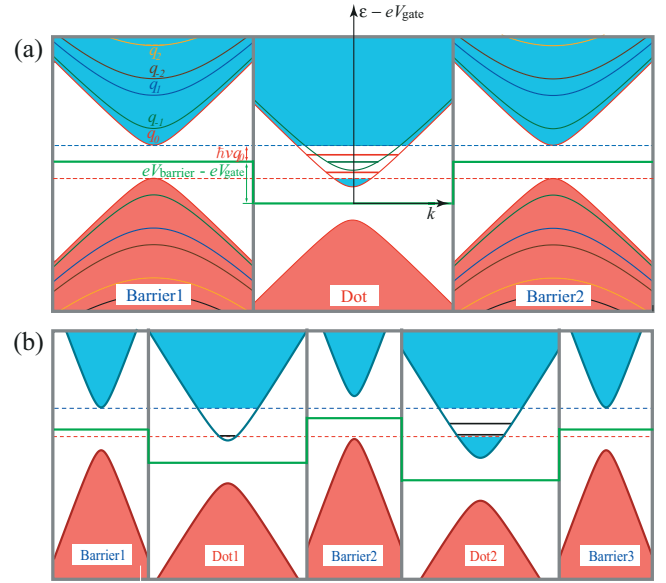


FIG. 3: (a) Energy bands for two barrier regions and a single dot. The red area marks a continuum of states in the valence bands and the blue area marks a continuum of states in the conduction bands. In the barrier regions, we indicate the energy bands of the quantized modes due to transverse confinement. All modes are non-degenerate solutions in valley space. They come pairwise in a sense that always two of them are separated by a distance $\hbar\nu q_0$ in energy space. In the figure, this is illustrated for the energy levels corresponding to wave vectors q_0 and q_{-1} as well as q_1 and q_{-2} . In the dot region, the electric confinement in longitudinal direction yields an additional level structure, i.e. the one shown in Fig. 2. For clarity, we only show the dot levels that are located in the gap of the barrier regions and are, therefore, bound states. In the figure, we choose to present a situation with three bound states in total: Two of them are of the $n = 0$ series (straight red lines in the center region) and a single one is of the $n = -1$ series (straight green line in the center region). (b) Energy bands for a double dot setup. A single bound state (straight black line) is shown in the conduction band of the left dot and two bound states are shown in the conduction band of the right dot. They are coupled via the continuum in the valence band of the central barrier. Thus, the long-range coupling is enabled by the Klein paradox.

a non-trivial requirement in a graphene structure, as in bulk graphene, there is a two-fold orbital (“valley”) degeneracy of states around the points \mathbf{K} and \mathbf{K}' in the first Brillouin zone. This valley degeneracy is lifted in our case of a ribbon with *semiconducting armchair edges*, and the ground-state solutions determined by Eq. (9) are in fact non-degenerate. The magnitude of the exchange coupling within a Hund-Mulliken model is [7] $J = (-U_H + (U_H^2 + 16t_H^2)^{1/2})/2 + V$, where t is the tunneling (hopping) matrix element between the left and right dot, U is the on-site Coulomb energy, and V is the direct exchange from the long-range (inter-dot) Coulomb interaction. The symbols t_H and U_H indicate that these quantities are renormalized from the bare values t and U by the inter-dot Coulomb interaction. For $t \ll U$ and neglecting the long-ranged Coulomb part, this simplifies to the Hub-

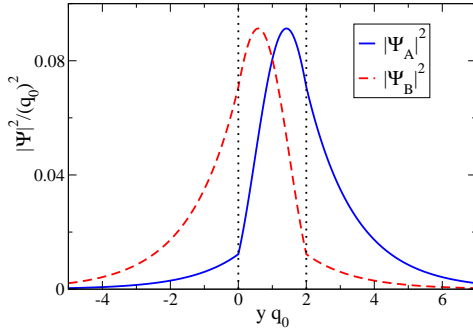


FIG. 4: Normalized squared wave functions $|\Psi_A|^2 = |\Psi_A^{(K)}|^2 = |\Psi_A^{(K')}|^2$ and $|\Psi_B|^2 = |\Psi_B^{(K)}|^2 = |\Psi_B^{(K')}|^2$ for the bound state solution for the parameter choice $e(V_{\text{barrier}} - V_{\text{gate}}) = 0.6\hbar v q_0$, and $q_0 L = (\pi/3)L/W = 2$ (indicated by the arrow in Fig. 2). The corresponding energy is given by $\varepsilon \approx 1.31 \cdot \hbar v q_0$. The dotted lines indicate the dot region $0 \leq y \leq L$.

band model result $J = 4t^2/U$ where t is the tunneling (hopping) matrix element between the left and right dot and U is the on-site Coulomb energy. In the regime of weak tunneling, we can estimate $t \approx \varepsilon \int \Psi_L^\dagger(x, y) \Psi_R(x, y) dx dy$, where $\Psi_{L,R}(x, y) = \Psi(x, y \pm (d + L)/2)$ are the ground-state spinor wave functions of the left and right dots and ε is the single-particle ground state energy. Note that the overlap integral vanishes if the states on the left and right dot belong to different transverse quantum numbers $q_{n_L} \neq q_{n_R}$. For the ground state, we have $n_L = n_R = 0$, and the hopping matrix element can be estimated for $d \gtrsim L$ as

$$t \approx 4\varepsilon \alpha_0 \delta_0^* W dz_{0,k} \exp(-d|k|), \quad (10)$$

where α_0 and δ_0 are wave function amplitudes (with dimension 1/length) specified in Eq. (4). As expected, the exchange coupling decreases exponentially with the barrier thickness, the exponent given by the “forbidden” momentum k in the barrier, defined in Eq. (6). The amplitude t can be maximized by tuning to a bound-state solution, where $|\varepsilon - eV_{\text{barrier}}|$ approaches $\hbar v q_0$ (from below). Then, $d|k| < 1$. Such a fine-tuning can be easily achieved in graphene quantum dots, where the small band gap allows to sweep through it and,

therefore, to use conduction and valence band states (of the barrier region) to couple quantum dots, see Fig. 3(b). Remarkably, this opens up the possibility for long distance coupling of electron spins because, in the limit $|\varepsilon - eV_{\text{barrier}}| \rightarrow \hbar v q_0$, the coupling t depends only weakly on the distance d between the quantum dots. However, already for bound state solutions with $|k|d > 1$, a coupling over a length exceeding several times the dot size is possible. We find, for instance, a solution, where $|k|d = 4$, $d = 10L$, and the coupling can still be as large as $t \approx 0.06\varepsilon$ for highly localized qubits.

The values of t , U , and J can be estimated as follows. The tunneling matrix element t is a fraction of $\varepsilon \approx 30 \text{ meV}$ (for a width of $W \approx 30 \text{ nm}$), we obtain that $t \approx 1 \dots 5 \text{ meV}$. The value for U depends on screening which we can assume to be relatively weak in graphene [21], thus, we estimate, e.g., $U \approx 10 \text{ meV}$, and obtain $J \approx 0.4 \dots 6 \text{ meV}$.

For the situation with more than two dots in a line, it turns out that we can couple any two of them with the others being decoupled by detuning. This is done by shifting the gates of the decoupled dots such that the bottom of the conduction band of these dots lies a little bit above the energy levels of the two dots that are coupled. This is a unique feature of graphene quantum dots due to the small and highly symmetric band gap, which is not known to exist for other semiconducting materials. The availability of non-local interactions is important in the context of quantum error correction, as it raises the error threshold for fault-tolerant quantum computation [27].

In conclusion, we have proposed a setup to form spin qubits in quantum dots based on graphene nanoribbons with semiconducting armchair boundary conditions. For such a system, we have calculated bound states of a tunable dot and outlined how two-qubit gates can be realized. We expect very long coherence times for such spin qubits since spin-orbit coupling and hyperfine interaction are known to be weak in carbon. Furthermore, we have found that the high flexibility in tuning graphene quantum dots in combination with conduction band to valence band tunneling based on the Klein paradox allows for long distance coupling of electron spins. Therefore, we propose a system which can serve as the fundamental building block for scalable and fault-tolerant quantum computing.

We thank H.A. Fertig for discussions and acknowledge support from the Swiss NSF, NCCR Nanoscience, DARPA, ONR, and JST ICORP.

-
- [1] D. Loss and D.P. DiVincenzo, Phys. Rev. A **57**, 120 (1998).
[2] J.M. Elzerman, *et al.*, Nature **430**, 431 (2004).
[3] R. Hanson, *et al.*, Phys. Rev. Lett. **94**, 196802 (2005).
[4] J.R. Petta, *et al.*, Science **309**, 2180 (2005).
[5] F.H.L. Koppens, *et al.*, Nature **442**, 766 (2006).
[6] V.N. Golovach, A.V. Khaetskii, and D. Loss, Phys. Rev. Lett. **93**, 016601 (2004).
[7] G. Burkard, D. Loss, and D.P. DiVincenzo, Phys. Rev. B **59**, 2070 (1999).
[8] A.V. Khaetskii, D. Loss, and L. Glazman, Phys. Rev. Lett. **88**, 186802 (2002).
[9] W.A. Coish and D. Loss, Phys. Rev. B **70**, 195340 (2004).
[10] A.C. Johnson, *et al.*, Nature **435**, 925 (2005).
[11] F.H.L. Koppens, *et al.*, Science **309**, 1346 (2005).
[12] H. Min, *et al.*, Phys. Rev. B **74**, 165310 (2006).
[13] K.S. Novoselov, *et al.*, Science **306**, 666 (2004).
[14] K.S. Novoselov, *et al.*, Nature **438**, 197 (2005).
[15] Y. Zhang, Y.-W. Tan, H.L. Stormer, and P. Kim, Nature **438**, 201 (2005).
[16] V.V. Cheianov and V.I. Falko, Phys. Rev. B **74**, 041403(R) (2006).
[17] N. Dombay and A. Calogeracos, Phys. Rep. **315**, 41 (1999).

- [18] M.I. Katsnelson, K.S. Novoselov, and A.K. Geim, *Nature Phys.* **2**, 620 (2006).
- [19] J.W. McClure, *Phys. Rev.* **104**, 666 (1956).
- [20] G.W. Semenoff, *Phys. Rev. Lett.* **53**, 2449 (1984).
- [21] D.P. DiVincenzo and E.J. Mele, *Phys. Rev. B* **29**, 1685 (1984).
- [22] P.G. Silvestrov and K.B. Efetov, *cond-mat/0606620*.
- [23] J. Nilsson, A.H. Castro Neto, F. Guinea, and N.M.R. Peres, *cond-mat/0607343*.
- [24] A. De Martino, L. Dell'Anna, and R. Egger, *cond-mat/0610290*.
- [25] L. Brey and H.A. Fertig, *Phys. Rev. B* **73**, 235411 (2006).
- [26] J. Tworzydlo, B. Trauzettel, M. Titov, A. Rycerz, and C.W.J. Beenakker, *Phys. Rev. Lett.* **96**, 246802 (2006).
- [27] K.M. Svore, B.M. Terhal, and D.P. DiVincenzo, *Phys. Rev. A* **72**, 022317 (2005).
- [28] At this point, we are only interested in the orbital structure of the wave function. The spin degree of freedom is neglected until the final part, where we discuss the Heisenberg exchange coupling for spins in tunnel-coupled quantum dots.
- [29] If we relax this assumption, we can show that for the case $z_{0,k} = z_{0,\tilde{k}}$ only a single solution to Eq. (7) exists, namely $z_{0,\tilde{k}} = 1$, which implies that $\tilde{k} = 0$. The corresponding wave function to this solution vanishes identically.